



Evidence for potential functionality of nuclearly-encoded humanin isoforms

Marek Bodzioch ^{a,*}, Katarzyna Lapicka-Bodzioch ^a, Barbara Zapala ^a, Wojciech Kamysz ^b,
Beata Kiec-Wilk ^a, Aldona Dembinska-Kiec ^a

^a Department of Clinical Biochemistry, Collegium Medicum, Jagiellonian University, Kopernika 15a, 31-501 Krakow, Poland

^b Department of Inorganic Chemistry, Faculty of Pharmacy, Medical University of Gdansk, Gdansk, Poland

ARTICLE INFO

Article history:

Received 23 February 2009

Accepted 19 May 2009

Available online 27 May 2009

Keywords:

Humanin

Apoptosis

Mitochondrial function

Genetic variation

Beta-carotene

ABSTRACT

Humanin (HN) is a recently identified neuroprotective and antiapoptotic peptide derived from a portion of the mitochondrial *MT-RNR2* gene. We provide bioinformatic and expression data suggesting the existence of 13 *MT-RNR2*-like nuclear loci predicted to maintain the open reading frames of 15 distinct full-length HN-like peptides. At least ten of these nuclear genes are expressed in human tissues, and respond to staurosporine (STS) and beta-carotene. Sequence comparisons of the nuclear HN isoforms and their homologues in other species reveal two consensus motifs, encompassing residues 5–11 (GFS/NCLLL), and 14–19 (SEIDLPS). Proline vs serine in position 19 may determine whether the peptide is secreted or not, while threonine in position 13 may be important for cell surface receptor binding. Cytoprotection against the STS-induced apoptosis conferred by the polymorphic HN5 variant, in which threonine in position 13 is replaced with isoleucine, is reduced compared to the wild type HN5 peptide.

© 2009 Elsevier Inc. All rights reserved.

Introduction

Humanin (HN) is a recently discovered 24-amino acid peptide with cytoprotective properties, involving several distinct mechanisms. It was initially identified as a neuroprotective factor against Alzheimer's disease (AD)-specific triggers [1]. Neuroprotection is mediated through the inhibition of the c-Jun (JUN) N-terminal kinase (JNK) [2], tyrosine kinases and STAT3 or STAT3-related transcription factors [3], and/or extracellular signal-regulated kinase (ERK [MAPK1]) pathway [4], and requires the interaction of HN dimers [5] with cell surface receptors [6]. Although HN is a high-affinity ligand of G-protein coupled formyl peptide receptors, formyl peptide receptor-like 1 and 2 (FPRL1 [FPR2] and FPRL2 [FPR3]) [7], and was shown to protect FPRL1 (FPR2)-expressing neuroblasts from amyloid-beta₄₂(Aβ₄₂)-induced apoptosis [8], the exact mechanisms linking FPRL1 (FPR2) and FPRL2 (FPR3) with HN-mediated neuroprotection are unknown, and additional HN-specific receptors have been postulated [3]. Neuroprotection may partially be attributed to the interaction of HN with insulin-like growth factor-binding protein 3 (IGFBP-3). IGFBP-3 was also suggested to serve as the HN transporter in both the circulation and tissues, reminiscent of its carrier function for the insulin-like growth factors (IGFs) [9]. The cytoprotective effects of HN are not confined to neurons, and involve other components of the brain (rescue of human cerebrovascular smooth muscle cells from Aβ-induced toxicity [10]) as well as extraneural tissues (prolonged survival of serum-deprived rat

pheochromocytoma cells [11], and human lymphocytes [12] and muscular cells [13]). Delayed apoptosis of serum-deprived leukemia K562 cells was found dependent upon the inhibition of the p38 signaling pathway [14]. Whereas HN secretion and extracellular receptor-binding seem critical for neuroprotection, HN is also a potent intracellular inhibitor of apoptosis, interacting with the members of the BCL2/BAX proapoptotic protein family, BAX [15], BID, tBID [16], and BIM_{EL} (BCL2L11) [17], and interfering with the activation of this pathway. Moreover, there is some evidence suggesting that HN can act directly on the mitochondria to increase the ATP production, independent of BAX inactivation [13]. The intracellular HN level may be controlled, at least in part, by the ubiquitin-mediated protein degradation pathway through the interaction with the tripartite motif protein 11 (TRIM11) [18].

Increased expression of the HN peptide observed in the AD brains [1], synovial cells affected with the diffuse type pigmented villonodular synovitis [19], and skeletal muscles from patients with mitochondrial disorders [20,21] suggests that HN is part of the physiological mechanisms promoting cell survival under stressful conditions, such as neurodegeneration, inflammation, or energy deficiency. Consistently, the exogenous administration of the more potent synthetic HN derivative, Gly14-HN (HNG), improved experimentally-induced impairments of learning and memory [22], spatial memory [23], as well as behavioral deficits [24] in rodents, and reduced the volume of cerebral infarct in a murine model of stroke [4,25]. These *in vivo* effects of HNG may involve the inhibition of neuroinflammation [24], and activation of the PI3K/Akt pathway [25].

Further modifications of HNG led to the creation of even more active analogues, including AGA-(C8R)HNG [26] and its derivatives, as

* Corresponding author. Fax: +48 12 421 4073.

E-mail address: mb22@mp.pl (M. Bodzioch).

well as colivelin, formed by the attachment of the activity-dependent neurotrophic factor [27]. These new peptides were shown to improve quinuclidinyl benzilate-induced spatial memory impairment in rats [28], and prolong survival of the amyotrophic lateral sclerosis model mice [29].

While there is compelling evidence for the endogenous HN synthesis [30], the exact location of the gene (or genes) encoding the peptide has not been determined conclusively. The originally identified 1567-base cDNA containing the open reading frame (ORF) of HN is 99% identical with a fragment of the *MT-RNR2* gene, coding for the 16S subunit of the mitochondrial rRNA [1], which gave rise to speculations that HN might be translated from the mitochondrial 16S rRNA with a polyA tail [26]. Should the translation occur in the mitochondrion rather than cytoplasm, the usage of the mitochondrial genetic code would result in a premature stop codon and slightly shorter peptide, lacking the last three carboxy-terminal amino acids. However, even such abbreviated peptide was fully functional in regard to the inhibition of the BAX-mediated proapoptotic pathway [15]. Alternatively, HN could be encoded within one or more of the nuclear regions with 92–95% similarity to the original HN cDNA, dispersed in multiple copies throughout the human genome [1,15],

though they have not been analyzed systematically for their coding potential so far.

In this report, we present bioinformatic evidence for the existence of at least 13 distinct human nuclear loci that maintain the ORFs for a host of putative full-length (i.e. 24-amino acid-long or longer) HN-like peptides. We also provide gene expression data showing that at least ten of them might be functional genes regulated in a tissue- and factor-specific manner. Additionally, we synthesized two of these peptides and proved their antiapoptotic properties.

Results

Putative HN isoforms encoded by the nuclear genes

The BLASTN searches yielded 28 nuclear sequences highly homologous with the *MT-RNR2* HN ORF dispersed throughout the human genome. Following the translation with the standard genetic code 13 of them proved to maintain the ORFs of full-length HN-like peptides. The remaining 15 sequences apparently could not generate functional peptides due to a premature stop codon (most often at codon 4) or lack of a consensus translation start site (ATG). The






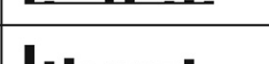


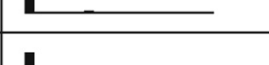
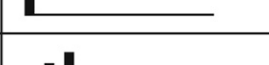


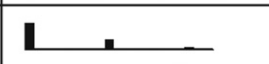
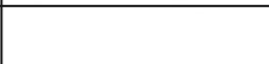

Gene	Isoform	Cytogenetic location and contig No	Chromosomal position	Primer sequences	
<i>MT-RNR2</i>	HNM	mtDNA NC_001807.4	<i>MT-RNR2</i>	F: aatcactgttccttaaataggacc R: gaaccctcgtggagccatt	
<i>MTRNR2L1</i>	HN1	17p11.2 NT_024862.13	between <i>UBBP4</i> and <i>LOC729490</i>	F: cactgtccttaaataggactgtc R: agctgaaccctcgtggagc	
<i>MTRNR2L2</i>	HN2	5q14.1 NT_006713.14	within intron 2 of <i>DHFR</i>	F: tctcatggataggccaattcactg R: ggacatcctgacatttagtgatct	
<i>MTRNR2L3</i>	HN3	20q13.31 NT_011382.9	within intron 4 of <i>RAE1</i>	F: tgaatgaatggccacaogaa R: tcaatgggtgaaagtaagagacgct	
<i>MTRNR2L4</i>	HN4	16p13.3 NT_037687.4	between <i>ZNF434</i> and <i>OR2C1</i>	F: gggtcagctgtctctacttcag R: tctcatggataggccaattcactg	
<i>MTRNR2L5</i>	HN5	10q21.1 NT_006583.18	between <i>PCDH15</i> and <i>LOC389970</i>	F: aatggccacaccagggtt R: tcaattcactggtgaaagtaagagac	
<i>MTRNR2L6</i>	HN6	7q34 NT_007914.14	T cell receptor beta locus	F: tgtctctactccaaccaggaac R: cataggatctctcaatctatttcatgtt	
<i>MTRNR2L7</i>	HN7	10p11.21 NT_006705.15	between <i>ZNF248</i> and <i>LOC219752</i>	F: ggcacacaggagggttg R: gataggccaattccctgattaaaagtaag	
<i>MTRNR2L8</i>	HN8	11p15.3 NT_008237.17	between <i>RNF141</i> and <i>AMPD3</i>	F: cctgcccgaagaggc R: ccatagggtctctcgtctgttatac	
<i>MTRNR2L9</i>	HN9	6q11.1 NT_007299.12	close to 3' end of <i>LOC727798</i>	F: ttcagctgtctctacttcaaccac R: gcctctcacgggcaggt	
<i>MTRNR2L10</i>	HN10	Xp11.21 NT_011830.14	between <i>PAGE5</i> and <i>FAM104B</i>	F: cagggaatgacccatccgc R: ctgcttattgtttatataccgc	
<i>MTRNR2L11</i>	HN11	1q42.3 NT_004838.17	between <i>ZP4</i> and <i>LOC339535</i>	F: gaaattgacctatccgtgaaggg R: ggtctcttctattgtttataccca	
<i>MTRNR2L12</i>	HN12	3q11.2 NT_005612.15	close to 5' end of <i>LOC644082</i>	F: gcgggcataacatagcaagact R: ttgagaaaaactgctcagtaacatg	
<i>MTRNR2L13</i>	HN13	4q26 NT_016354.18	between <i>LOC645368</i> and <i>LOC344978</i>	F: tctctactttaaactcagtaaatgacctat R: ttgtttatataccgctcttca	

Fig. 1. Genomic localization, specific primer sequences for quantitative RT-PCR, and tissue expression profiles of the putative nuclear *MT-RNR2*-like genes encoding HN isoforms. Black columns indicate expression levels of each isoform in different tissues as a percent of the rate in the testis, which was used as a comparator and considered 100%. The isoforms are ordered according to the decreasing overall amount of the transcript in the testis, though the expression analysis was not specifically designed to compare the isoforms between each other, and this is only an approximation. The isoforms encoded by *MTRNR2L11*, *MTRNR2L12*, and *MTRNR2L13* were not expressed in any of the studied tissues. All names of the putative novel peptide-coding genes were consulted with and approved by Human Genome Nomenclature Committee.

approximate chromosomal locations and tissue expression profiles (see below) of all the *MT-RNR2*-like genes with a coding potential are shown in Fig. 1, while the predicted amino acid sequences of their putative products are aligned in Fig. 2.

The predicted HN peptides show a high degree of conservation with amino acid positions 1, 6, 8, 9, 10, 11, 17, 18, 21, and 22 identical in all the isoforms, including the prototype mitochondrial HN (HNM) encoded by the *MT-RNR2* gene. Well conserved are also positions 5, 7, 15, 16, and 19, which only occur in two variants. The most variable (three or more variants) are amino acids 2, 3, 4, 12, 13, 14, 20, 23, and 24. Isoforms HN2 and HN4 encoded by the *MTRNR2L2* and *MTRNR2L4* genes, respectively, are predicted to have four additional carboxy-terminal amino acids. Despite a high degree of homology every isoform has a unique amino acid sequence except for identical HN8 and HN12 encoded by the *MTRNR2L8* and *MTRNR2L12* genes, respectively. However, there is a polymorphic site (rs7350541) within *MTRNR2L8*, predicted to cause the Ser12Leu amino acid exchange, and produce a peptide sequence identical to the prototype HNM. We identified another polymorphic site (rs11004928) within the putative *MTRNR2L5* gene, changing threonine to isoleucine in amino acid position 13 (Thr13Ile) of HN5. Taking into account these polymorphic variants, there might be as many as 15 distinct HN peptides encoded by *MT-RNR2*-like nuclear genes.

Homologues of nuclear *MT-RNR2*-like genes in other species

We identified 14 putative full-length chimpanzins, i.e. HN homologues in the chimpanzee, encoded in its nuclear genome (Fig. 3). They are all well-conserved with some positions showing moderate variability in a pattern very similar to that in humans. There is a considerable overlap between human and chimpanzee *MT-RNR2*-like genes as evidenced by the phylogenetic analysis (Fig. 4). Most of these genes are located in syntenic chromosomal regions and have the same or nearly-identical amino acid sequences in both species. However, there are also important differences. Human *MTRNR2L1*, *MTRNR2L2*, *MTRNR2L6*, and *MTRNR2L9* genes do not have their counterparts in the chimpanzee genome, while there are four additional genes in the chimpanzee, which are absent in humans, including (PANTR)*MTRNR2L14*, (PANTR)*MTRNR2L15*, (PANTR)*MTRNR2L16*, and the unique multi-copy (PANTR)*MTRNR2L17* in sex chromosome Y predicted to encode a peptide with an extra asparagine between the conserved residues 17 and 18 (PANTR)*MT-RNR2*, (PANTR)*MTRNR2L2*, (PANTR)*MTRNR2L6*, (PANTR)*MTRNR2L8*, and (PANTR)*MTRNR2L14* apparently encode the same peptide identical with HN8 and HN12.



Fig. 2. Multiple sequence alignment of the predicted HN peptides. Alignment was done by ClustalW and rendered graphically by BOXSHADE 3.21. Identical and similar amino acids are highlighted in black and gray, respectively. "M" indicates the mitochondrial isoform, while numbers refer to chromosomes, in which the nuclear isoforms are located. The two HN loci in chromosome 10 are distinguished by "a" and "b". The two polymorphic variants of HN10b are indicated as T13 and I13. The isoforms that were not expressed in any of the studied tissues are marked with #.

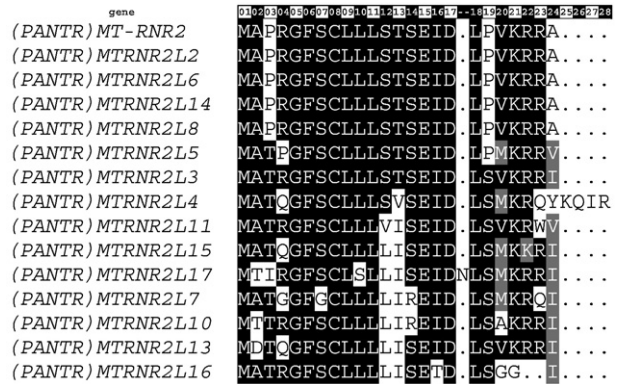


Fig. 3. Multiple sequence alignment of the predicted chimpanzin peptides encoded by (PANTR)*MT-RNR2* and putative (PANTR)*MT-RNR2*-like nuclear genes. Alignment was done by ClustalW and rendered graphically by BOXSHADE 3.21. Identical and similar amino acids are highlighted in black and gray, respectively. There are multiple tandemly repeated copies of *MTRNR2L17* in chromosome Y.

In the nuclear genome of the Rhesus monkey (*Macaca mulatta*), we found as many as 20 different *MT-RNR2*-like loci with a coding potential. The predicted Rhesus peptides differ from the HNs and chimpanzins more than the latter two between themselves but share a similar pattern of conserved residues (Fig. 5). Interestingly, the mitochondrial isoform lacks a consensus translation initiation site (either nuclear or mitochondrial), though the normal ATG codon is present in the mitochondrial gene of the closely related Barbary macaque (*Macaca sylvanus*). Unlike in primates, the nuclear *MT-RNR2*-like loci seem very infrequent in other organisms; we only were able to identify single nuclear loci with a coding potential in some mammalian species, including a cow, a dog, and a mouse (Fig. 6). However, the mitochondrial sequences maintaining the ORFs of peptides similar to HN are relatively well-conserved in mtDNA, where they can be traced down the whole evolutionary tree. Similarly to the Rhesus monkey, mice lack a valid translation start site within the mitochondrial homologue, though they have a nuclear gene predicted to code for a peptide with 13 additional carboxy-terminal amino acids. On the other hand, rats apparently have no coding nuclear genes but possess a mitochondrial gene with the consensus ATG translation start site. Dependent upon the usage of the mitochondrial vs standard genetic code, the putative mitochondrial homologues in a cow, a dog, and a rat (and possibly a mouse, if the lack of a valid translation start site is neglected) could produce alternative products distinguished by the presence or absence of the carboxy-terminal tail of between 11 and 23 amino acids.

Tissue expression profiles of the *MT-RNR2*-like genes

Specific mRNA species of ten of the 13 putative nuclear *MT-RNR2*-like genes were detectable in one or more of the studied tissues (Fig. 1). We could not confirm the expression of *MTRNR2L11*, *MTRNR2L12*, or *MTRNR2L13*. The remaining genes, including *MT-RNR2*, were generally highly expressed in the testis, kidney, heart, skeletal muscles, and brain, and had low expression in the liver, thyroid gland, or bone marrow. The most consistent feature was high expression of all the isoforms in the testis. *MT-RNR2*, *MTRNR2L1*, *MTRNR2L8*, and *MTRNR2L9* were notable for high expression in the kidney and heart muscle, which matched or exceeded that in the testis. *MTRNR2L7* was only detectable in the testis, while *MTRNR2L5* was additionally expressed in the brain, *MTRNR2L6* – in skeletal muscles, and *MTRNR2L10* – in the mature brain and thyroid gland. *MTRNR2L8* was not expressed in skeletal muscles despite high expression in the heart. Since the analysis was primarily designed to obtain the isoform-specific patterns of relative expression in different tissues, direct comparison of the isoforms between each other could only be used for

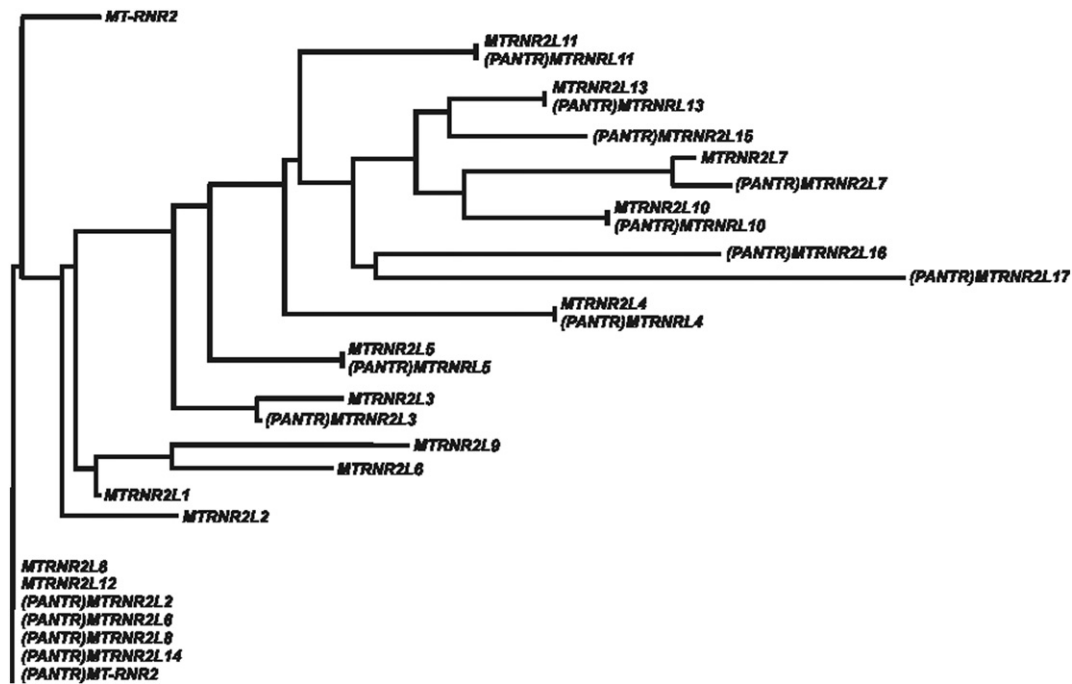


Fig. 4. The phylogenetic tree of the putative genes encoding humanin and chimpanzin peptides. *There are multiple tandemly repeated copies of (PANTR)MTRNR2L11 in chromosome Y.

approximate estimation. Nevertheless, it was apparent that in all the studied tissues the expression of *MT-RNR2* was considerably higher than of any of the nuclear isoforms. In the testis, the difference ranged roughly from 100-fold (*MT-RNR2* compared to *MTRNR2L1*) up to 250,000-fold (*MT-RNR2* compared to *MTRNR2L10*).

Expression response to pro- and antiapoptotic stimuli in human umbilical vein endothelial cells (HUVECs)

Since endothelial cells were not included in the standardized human RNA panel described above, we first measured the baseline expression of the putative *MT-RNR2*-like genes in HUVECs, and found that it was high for all the isoforms except for *MTRNR2L11*, *MTRNR2L12*, and *MTRNR2L13*, which apparently were not expressed, similar to the other studied tissues.

STS (Fig. 7A)

At 6 h, the proapoptotic STS downregulated all of the isoforms leading to a maximum six-fold decrease in the expression of *MTRNR2L2*. However, for *MT-RNR2* and *MTRNR2L4*, this effect was small and not significant. After 24 h, the trend was reversed and all the genes became upregulated compared to the baseline with the strongest effect (eight-fold or more) noted for *MTRNR2L3*, *MTRNR2L6*, *MTRNR2L8*, and *MTRNR2L9* (Fig. 7A).

Beta-carotene (Fig. 7B)

In HUVECs, beta-carotene inhibits BAX and acts as an antiapoptotic factor [32]. Following a six-hour incubation with this agent all of the genes became downregulated (2–8-fold) except for *MTRNR2L2*, whose expression increased eight-fold. At 24 h, *MT-RNR2*, *MTRNR2L4*, and *MTRNR2L5* remained downregulated, while *MTRNR2L2* decreased to the baseline. The expression of the remaining genes increased, either returning to the baseline (*MTRNR2L6*, *MTRNR2L7*, *MTRNR2L8*, *MTRNR2L9*), or rising more than eight-fold above the baseline (*MTRNR2L3*, *MTRNR2L10*) (Fig. 7B).

Selection of HN peptides for functional studies

In order to prove the biological activity of peptides encoded by the nuclear genes we synthesized and tested two of them. We selected the

polymorphic variants of HN5, encoded by the *MTRNR2L5* gene, differentiated by threonine or isoleucine in amino acid position 13. This selection was based on: 1) evidence that Thr13 may be critical for binding with cell surface receptors and neuroprotective activity [31,32], and 2) the fact that Thr13Ile HN5 polymorphism represents a natural genetic variance, and thus may be relevant to human health. However, before undertaking the functional tests, we estimated the occurrence of both variants in the general population to rule out a very low frequency of a minor allele (see the next section). In addition to Thr13- and Ile13-HN5, we also synthesized the high-activity HNG and prototype HNM peptides as controls.

Genotyping the *HN10b* gene

Among the 93 healthy adult unrelated individuals 34 (36.5%) were homozygous for Thr13-HN5, 13 (14.0%) were homozygous for Ile13-HN5, while the remaining 46 (49.5%) were heterozygous. Thus, both alleles are common in the general population with frequencies of 61.3% and 38.7% for the Thr13-HN5 and Ile13-HN5 variants, respectively.

Functional imaging

The 24-hour preincubation with HN peptides (HNG, HNM, Thr13-HN5, or Ile13-HN5; 4 μ M final conc.) protected HUVECs against the proapoptotic effects of STS, slowing the rate of the TMRM signal decrease (which reflected compromise of the mitochondrial function) and delaying morphological changes of the cells. Fig. 8 illustrates changes of the densitometry sum parameter (DSP), which is a composite measure of TMRM signal intensity and cell integrity (mean intensity \times ROI area, where ROI is a cytoplasmic region adjacent to an identifiable nucleus), 2 h following the administration of 0.01 μ M, 0.03 μ M and 0.1 μ M STS. The rate of DSP decrease with a rising STS concentration was similar in cells preincubated with HNG, HNM, and Thr13-HN5. However, in cells preincubated with Ile13-HN5 the DSP reduction was much greater, especially with the highest STS concentration.

When monitoring HUVECs with serial scans during the two-hour period of exposure to STS, we observed that STS-induced morphological

design, it should be emphasized that the quantitative RT-PCR is probably the only practical means of differentiating so closely related genes. While single nucleotide differences are usually enough to design specific primer sets, it would be very difficult (if not impossible) to raise antibodies with a matching degree of discriminating power. Moreover, in order to minimize the risk of sample contamination with genomic DNA or immature mRNA intermediates, we isolated total RNA from HUVECs, having first removed their nuclei, and, subsequently, incubating the RNA samples with DNases.

Nevertheless, the results of our functional experiments with two of these peptides, representing synthetic HN5 variants, suggest that they do possess biological activity, and the mRNA species detected in various cells may indeed reflect true cellular processes.

We recorded the highest expression of the nuclear *MT-RNR2*-like in the testis, heart, skeletal muscles, and brain, which is consistent with the earlier reports on HN [6]. However, each gene had its own specific tissue expression pattern, as reviewed in detail in Results and Fig. 1. We could not detect specific mRNA species of *MTRNR2L11*, *MTRNR2L12*, and *MTRNR2L13*. They may not be normally expressed in the studied tissues or are true pseudogenes. *MTRNR2L12* is predicted to have an identical amino acid sequence as *MTRNR2L8*, and may be silenced to avoid redundancy. The other two non-expressors are predicted to code for peptides with unique amino acids, Val12 in *MTRNR2L11* and Asp2 in *MTRNR2L13*, which do not occur in any of the other putative HN peptides, and might represent inactivating mutations.

HN was previously shown to be induced by proapoptotic stimuli, such as STS or serum deprivation [15], which act through the BAX-dependent pathways. We checked how STS affects the expression of *MT-RNR2* and *MT-RNR2*-like genes in HUVECs. After 24 h all the expressed genes were uniformly upregulated consistent with the cell survival activity mediated by both the intracellular (the Ser19 group) and extracellular (the Pro19 group) mechanisms. Surprisingly, the initial response after 6 h was quite opposite and was characterized by a decrease in expression of all the isoforms compared to the baseline. These results suggest that acute insults may in fact compromise the HN activity and reduce the cell survival potential initially. Therefore, the HN-mediated protection may be more specific for prolonged processes, such as neurodegeneration, inflammation, nutrient deficiency, or chronic exposure to noxious stimuli. In a recent study, the administration of HNG resulted in the reduction of the infarct volume in a murine model of stroke [4]. It can be hypothesized that the exogenous HNG overcame the relative HN deficiency in acute brain ischemia.

Contrary to STS, the response to beta-carotene was quite varied. We showed previously that beta-carotene prevents apoptosis in HUVECs through the inhibition of the proapoptotic BAX [32], which is also a target for the antiapoptotic activity of HN. According to our speculations, the interaction with BAX might be mediated by some or all of the Ser19 isoforms, which may lack the ability to exit the cell and would remain in the cytoplasm. Noteworthy, the three nuclear *MT-RNR2*-like genes with the highest expression response to beta-carotene after 24 h, *MTRNR2L3* (>eight-fold increase), *MTRNR2L10* (>eight-fold increase), and *MTRNR2L4* (nearly four-fold decrease), actually belong to the Ser19 group. The link between beta-carotene and HN may also involve the nuclear retinoid receptors, RXR α , one of the targets of IGFBP3, which apparently is regulated by HN [9].

Our data are not enough to answer conclusively the original question whether HN is or is not synthesized within the mitochondria or can be translated from the mitochondrial mRNA on cytoplasmic ribosomes. In some organisms, such as the Rhesus monkey or mouse, the predicted mitochondrial gene lacks a valid translation initiation signal (with either the standard or mitochondrial genetic code usage), and would be unlikely to support the synthesis of a peptide. On the other hand, in all our mRNA expression experiments, *MT-RNR2* encoding for the prototype HNM was by far more activated than any of the nuclear *MT-RNR2*-like genes, and showed a moderate response to both STS and beta-carotene. However, the ORF of HNM is located within

a functional mtDNA gene producing rRNA molecules, some of which may have a polyA tail [26]. The presence of the polyA attachment need not mean these RNA molecules are actually translated, but may be responsible for their reverse transcription and amplification in the quantitative RT-PCR experiments. Therefore, the observed moderate changes in “expression” of the peptide-coding *MT-RNR2* may have in fact reflected variations of the levels of the mitochondrial rRNA. Moreover, the relative abundance of the mitochondrial rRNA containing the putative peptide-coding sequence could have effectively masked the existence of highly homologous but significantly less abundant nuclear *MT-RNR2*-like mRNA species. This would explain the apparent lack of sequences specific for the putative nuclear *MT-RNR2*-like genes in the EST databases. A more indirect argument against the peptide-coding potential of *MT-RNR2* could also be made, pointing to the fact that the synthesis of the peptide would have to be tightly linked with the levels of the mitochondrial rRNA. Although this possibility cannot be completely ruled out, especially as HN appears upregulated in the proapoptotic conditions, which are also likely to affect the mitochondria, it would be difficult to explain the multitude of functions ascribed to HN by a single gene lacking independent mechanisms of regulation.

Assuming, however, that the nuclear *MT-RNR2*-like genes are the true and only source of the HN peptides, one would have to admit that the HN homologues encoded by the nuclear genes might be the exclusive feature of the primates, or, at most, mammals. Multiple isoforms seem unique for humans and monkeys, while in other mammalian species there are only single nuclear *MT-RNR2*-like genes per genome. In the rat, we were not able to identify any nuclear sequences that would bear significant resemblance to *MT-RNR2*. However, despite the lack of direct evidence for the *in vivo* production of rattin (no peptide detection experiments have been reported), the predicted mitochondrial rat peptide with 15 extra residues not only replicated the HN protection against the AD-specific insults, but additionally showed protective activity toward excitotoxic neuronal death [37]. On the other hand, as mentioned before, there is likely no functional mitochondrial homologue in mice.

Materials and methods

Bioinformatic analysis

The human genome was searched with BLASTN (<http://www.ncbi.nlm.nih.gov/genome/seq/BlastGen/BlastGen.cgi?taxid=9606>) using the prototype cDNA sequence [1] derived from the *MT-RNR2* gene as a query. Each hit was assessed for a coding potential of a full-length peptide (24 amino acid-long or longer) and mapped according to the NCBI Build 36.2. A similar procedure was used to detect nuclear *MT-RNR2*-like sequences in other species.

Peptide synthesis

Peptides included in this study (HNG, HNM, Thr13-HN5, and Ile13-HN5) were synthesized manually in a microwave reactor by the solid-phase method using the 9-fluorenylmethoxycarbonyl (Fmoc) chemistry (Lipopharm.pl, Zblewo, Poland). The completeness of each coupling reaction was monitored by the chloranil test. The peptides were cleaved from the solid support by trifluoroacetic acid (TFA) in the presence of water (2.5%), and triisopropylsilane (2.5%) as scavengers. The cleaved peptides were precipitated with diethyl ether. The peptides were purified by solid-phase extraction using protocol described previously [38]. The resulting fractions of purity greater than 95–98% were tested by high performance liquid chromatography (HPLC) and thin layer chromatography (TLC). The peptides were also analyzed by matrix-assisted laser desorption/ionization-time-of-flight mass spectrometry (MALDI-TOF). The peptides dissolved well in water and were stored in stock 1 μ g/ml water solution without precipitation.

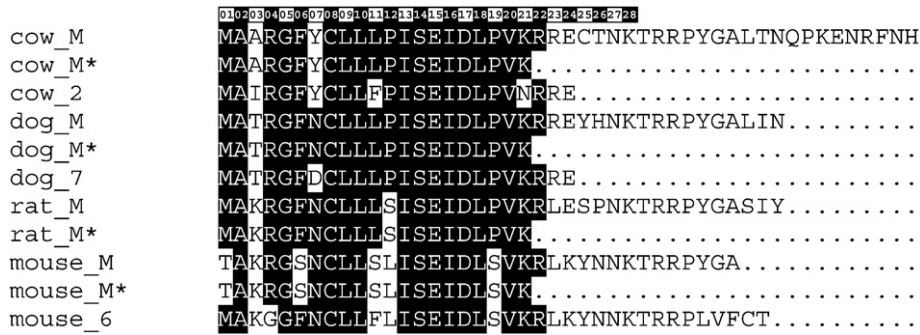


Fig. 6. Multiple sequence alignment of the predicted homologues of the HN peptides in non-primate mammalian species. “M” indicates the predicted long sequences of the putative mitochondrial isoforms translated with the mitochondrial genetic code, while “M*” refers to the shorter sequences obtained with the use of the standard genetic code. Numbers refer to chromosomes, in which the nuclear isoforms are located. There are apparently no nuclear HN homologues in the rat, while the putative mitochondrial isoform in the mouse does not have a consensus translation initiation signal.

Cell cultures

Human umbilical vein endothelial cells (HUVECs) were obtained from healthy donors by trypsinization of the umbilical vein.

For gene expression experiments, they were cultured for 6 and 24 h in fetal calf serum with 0.01 μM staurosporine (STS) or 3 μM beta-carotene (dissolved in 0.075% tetrahydrofuran [THF] and 0.075% ethanol). All-trans-beta-carotene was obtained from the chemical

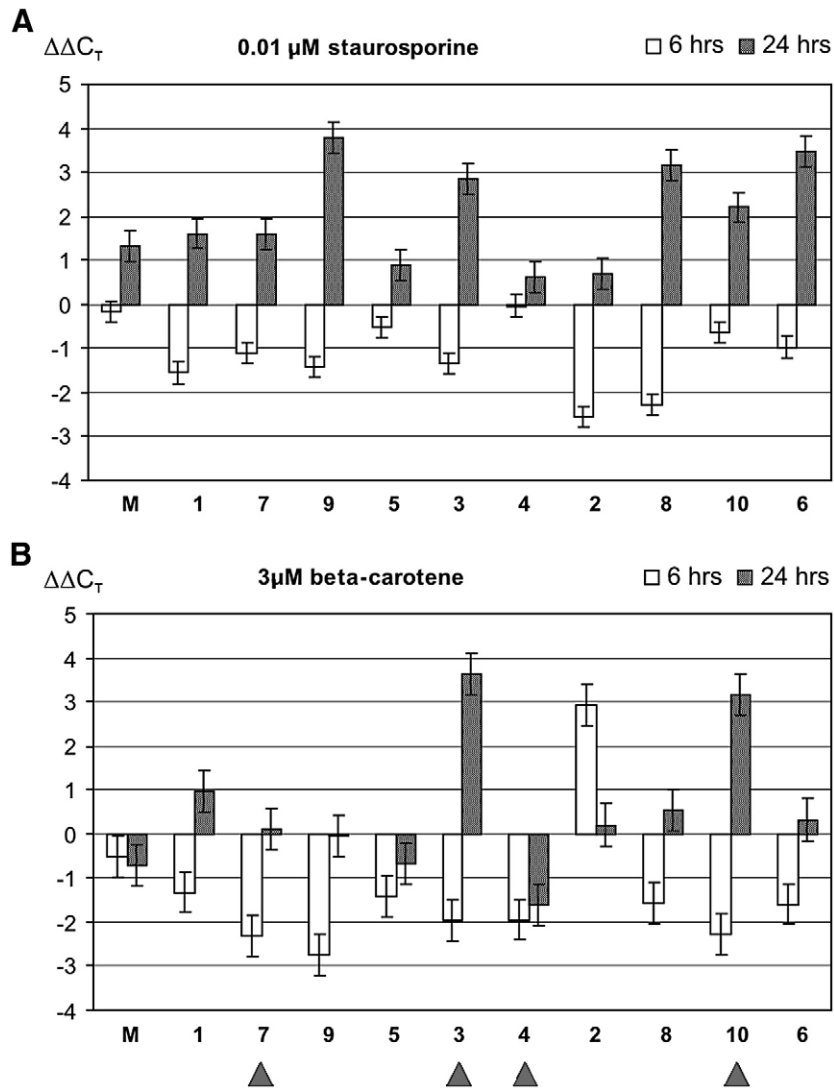


Fig. 7. The changes in relative expression rates of the HN isoforms in HUVECs following 6- and 24-hour exposure to 0.01 μM STS (A) or 3 μM beta-carotene (B). The results are represented as $\Delta\Delta C_T$, where one unit is equivalent to a two-fold change in expression. The isoforms from the Ser19 group, predicted to remain in the cytosol for the interaction with BAX and related proteins, are shown by arrowheads.

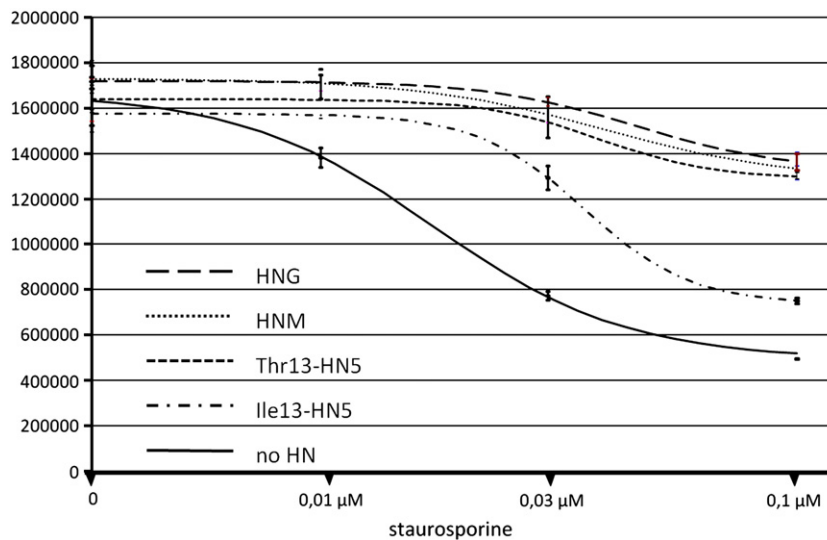


Fig. 8. Dose-response curves representing changes of the TMRM signal density sum parameter with increasing STS concentration in HUVECs preincubated with different HNs. The cells were incubated for 24 h with HNG, HNM, Thr13-HN5, and Ile13-HN5 (all HNs in 4 μM final conc.), or not pretreated with HN (no HN), and then exposed for 2 h to STS in 0.01 μM, 0.3 μM, or 0.1 μM concentration.

laboratories of Roche Vitamins AG (Kaiseraugst, Switzerland), while STS was purchased from Sigma-Aldrich (Poznan, Poland). In order to minimize beta-carotene oxidation and degradation all handling was performed in dimmed light and cooled conditions from small aliquots fractionated into argon-filled vials. In addition, THF and ethanol were filtered through the Alox columns to remove any traces of oxidizing substances. THF is a common solvent for beta-carotene but can be cytotoxic. We have shown previously that with the addition of ethanol the THF concentration can be reduced without compromising beta-carotene solubility, while the toxicity for HUVECs is minimized [32]. The induction and inhibition of apoptosis by STS and beta-carotene, respectively, was confirmed by Apo-ONE Homogeneous Caspase-3/7 Assay (Promega, Madison, WI, USA), consistent with the results of our earlier experiments [39]. Cell necrosis was excluded by the LDH assay (Cytotoxicity Detection Kit; Boehringer-Roche, Germany).

For live monitoring, HUVECs were seeded in 96-well clear bottom tissue culture plates for imaging applications (Becton Dickinson, Franklin Lakes, NJ, USA) at 10,000 cells per well to achieve 50% confluence and cultured for 24 h in fetal calf serum with different HN peptides, including HNG, HNM, Thr13-HN5, and Ile13-HN5, each in 4 μM final concentration. Subsequently, the cells were exposed to either 0.1 μM, 0.03 μM or 0.01 STS, and stained with tetramethylrho-

damine methyl ester (TMRM; final conc. 2 ng/μl) and Hoechst (final conc. 20 μM; both dyes from Molecular Probes, Carlsbad, CA, USA). Serial imaging was performed with an automated high-throughput microscope system, BD Pathway 855 High-Content Bioimager (Becton Dickinson, Franklin Lakes, NJ, USA) using the 20×/NA 0.75 objective. AttoVision 1.5 software was used to segment the cells into regions of interest, and changes in fluorescence intensity were analyzed with Image Data Explorer 2.2.15 (both software packages from BD Biosciences, San Jose, CA, USA).

Expression analysis

RNA sources

For the analysis of tissue expression profiles we used ten standardized high-quality RNA species selected from the Human Total RNA Master Panel II (Clontech Laboratories, Inc., Mountain View, CA, USA). In the STS/beta-carotene experiments, total RNA was isolated from the cells using the RNeasy Mini Kit (QIAGEN, Hilden, Germany). We applied the cytoplasmic protocol as described in the product manual in order to ensure the exclusive isolation of the mature mRNA species (without the admixture of nuclear mRNA intermediates or genomic DNA).

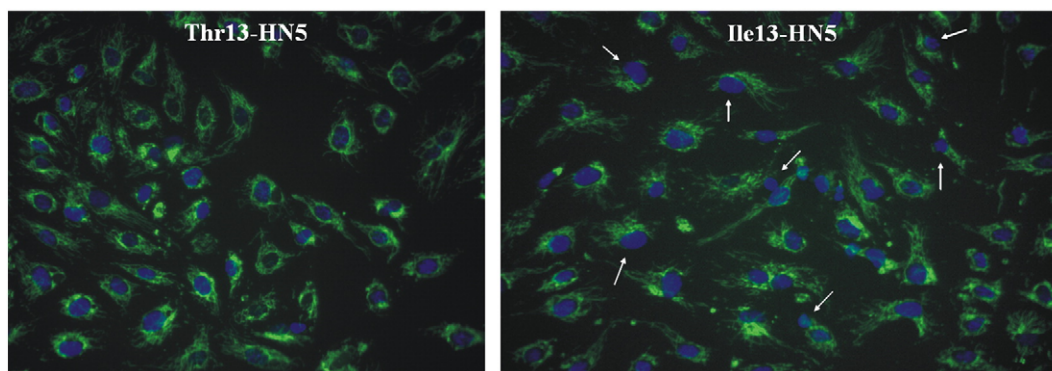


Fig. 9. Live images of the TMRM-stained HUVECs preincubated with Thr13- and Ile13-HN5 and exposed to STS. HUVECs preincubated for 24 h with 4 μM Thr13-HN5 (left panel) or 4 μM Ile13-HN5 (right panel) imaged live with BD Pathway 855 High-Content Bioimager (Becton Dickinson, Franklin Lakes, NJ, USA) 30 min following the exposure to 0.1 μM STS. The cells were stained with a marker of the mitochondrial function, TMRM (green), and a nuclear dye, Hoechst (blue). Magnification × 20. While the vast majority of cells pretreated with Thr13-HN5 seem intact, many of those incubated with Ile13-HN5 begin to show cytoplasm shrinkage. In normal HUVECs, mitochondria located in the cytoplasm symmetrically surround the nucleus, but are “shifted aside” exposing a “bare” nucleus (arrows in the right panel) as an early response to STS.

Primer design

We used Primer Express 2.0 Software (Applied Biosystems, Foster City, CA, USA) to design specific primer pairs amplifying each of the putative *MT-RNR2*-like genes maintaining the full ORF. Since the exact limits of the transcribed sequences have not been determined the primer pairs were located preferably within or very close to the putative coding regions (the most likely to be transcribed in an active gene). Despite a very high degree of homology it was possible to design a unique primer set for each *MT-RNR2*-like gene taking advantage of minor sequence differences between them, especially placing the oligo's final 3' nucleotide at the discriminating position (i.e. the one differing among the HN isoforms). Sequences of all primers are provided in Fig. 1. The same Primer Express 2.0 Software was used to design the primer pair for the calibrator (*GAPDH*; forward: CCAGCGCCCAATACGA; reverse: GCCAGCCGAGCCACATC). Specificity of the amplification products of all *MT-RNR2*-like genes and calibrator were confirmed by two-directional sequencing.

Amplification conditions

Forty ng aliquots of total RNA were reversely transcribed with oligo-dT primers using the Omniscript RT Kit (QIAGEN, Hilden, Germany) and PCR amplified on the DNA Engine Opticon® 2 Continuous Fluorescence Detection System (MJ Research, Inc., Waltham, MA, USA) using the QuantiTect SYBR Green PCR Kit (QIAGEN, Hilden, Germany) and standard recommended amplification conditions with the annealing temperature set to 59 °C. Each experimental point was measured in triplicate.

Data analysis

We analyzed the results according to the standard protocol for the comparative threshold cycle ($\Delta\Delta C_T$) method, using *GAPDH* as the endogenous calibrator. For the analysis of tissue expression profiles the expression rates of each gene in different tissues were compared to the testis and presented as a percentage value (the expression rate in the testis = 100%). The testis was selected as the comparator due to consistently high expression rates of most of the *MT-RNR2*-like genes there. The results of the exposure experiments were presented as $\Delta\Delta C_T$, which reflects a change in expression in response to an agent compared to an appropriate control (STS vs medium/beta-carotene vs medium with a solvent [ethanol and THF]).

Sequencing the *MTRNR2L5* gene

In order to establish the relative frequency of the *MTRNR2L5* variants we genotyped them by sequencing in 93 unrelated healthy adults, representing the general Polish population. The use of anonymized DNA samples was accepted by the local Bioethics Committee, and the patients provided informed consent to participate in genotype frequency and gene association studies.

DNA was isolated with the QIAamp DNA Blood Mini Kit (QIAGEN, Hilden, Germany), the *MTRNR2L5* putative coding sequence was amplified with the HotStarTaq Plus DNA Polymerase Kit (QIAGEN, Hilden, Germany), using the following primers: 5'-CCAATACAGTCATGCTCTAAGCAA-3' (forward) and 5'-CTCGTGATCCACCCACCT-3' (reverse). The PCR product was purified with QIAquick PCR Purification Kit (QIAGEN, Hilden, Germany) and sequenced with BigDye Terminator 3.1 Cycle Sequencing Kit (Applied Biosystems, Foster City, CA, USA). The products of cycle sequencing were cleared of unbound fluorescent dyes with BigDye X Terminator Purification Kit (Applied Biosystems, Foster City, CA, USA) and separated on the 3130xl Genetic Analyzer (Applied Biosystems, Foster City, CA, USA).

Acknowledgments

Authors are indebted to Ms Urszula Cialowicz and Ms Agnieszka Sliwa for their excellent work in cell culturing.

This work was supported by grants PBZ-KBN-124/P05/2004/4 and 2 P05A 006 29 from the Polish Ministry of Science and Higher Education.

References

- [1] Y. Hashimoto, et al., A rescue factor abolishing neuronal cell death by a wide spectrum of familial Alzheimer's disease genes and Abeta, *Proc. Natl. Acad. Sci. U. S. A.* 98 (2001) 6336–6341.
- [2] Y. Hashimoto, et al., Involvement of c-Jun N-terminal kinase in amyloid precursor protein-mediated neuronal cell death, *J. Neurochem.* 84 (2003) 864–877.
- [3] Y. Hashimoto, et al., Involvement of tyrosine kinases and STAT3 in Humanin-mediated neuroprotection, *Life Sci.* 77 (2005) 3092–3104.
- [4] X. Xu, C. Chua, J. Gao, R.C. Hamdy, B.H.L. Chua, Humanin is a novel agent against stroke, *Stroke* 37 (2006) 2613–2619.
- [5] Y. Hashimoto, et al., Humanin antagonists: mutants that interfere with dimerization inhibit neuroprotection by Humanin, *Eur. J. Neurosci.* 19 (2004) 2356–2364.
- [6] I. Nishimoto, M. Matsuoka, T. Nikura, Unravelling the role of humanin, *Trends Mol. Med.* 10 (2004) 102–105.
- [7] M. Harada, et al., N-Formylated humanin activates both formyl peptide receptor-like 1 and 2, *Biochem. Biophys. Res. Commun.* 324 (2004) 255–261.
- [8] G. Ying, et al., Humanin, a newly identified neuroprotective factor, uses the G protein-coupled formylpeptide receptor-like-1 as a functional receptor, *J. Immunol.* 172 (2004) 7078–7085.
- [9] M. Ikonen, et al., Interaction between the Alzheimer's survival peptide humanin and insulin-like growth factor-binding protein 3 regulates cell survival and apoptosis, *Proc. Natl. Acad. Sci. U. S. A.* 100 (2003) 13042–13047.
- [10] S.S. Jung, W.E. Van Nostrand, Humanin rescues cerebrovascular smooth muscle cells from A β -induced toxicity, *J. Neurochem.* 84 (2003) 266–272.
- [11] S. Kariya, et al., Humanin inhibits cell death of serum-deprived PC12h cells, *NeuroReport* 13 (2002) 903–907.
- [12] S. Kariya, N. Takahashi, M. Hirano, S. Ueno, Humanin improves impaired metabolic activity and prolongs survival of serum-deprived human lymphocytes, *Mol. Cell. Biochem.* 254 (2003) 83–89.
- [13] S. Kariya, M. Hirano, Y. Furiya, S. Ueno, Effect of humanin on decreased ATP levels of human lymphocytes harboring A3243G mutant mitochondrial DNA, *Neuropeptides* 39 (2005) 97–101.
- [14] D. Wang, et al., Humanin delays apoptosis in K562 cells by downregulation of P38 MAP kinase, *Apoptosis* 10 (2005) 963–971.
- [15] B. Guo, et al., Humanin peptide suppresses apoptosis by interfering with Bax activation, *Nature* 423 (2003) 456–461.
- [16] D. Zhai, et al., Humanin binds and nullifies Bid activity by blocking its activation of Bax and Bak, *J. Biol. Chem.* 280 (2005) 15815–15824.
- [17] F. Luciano, et al., Cytoprotective peptide humanin binds and inhibits proapoptotic Bcl-2/Bax family protein BimEL, *J. Biol. Chem.* 280 (2005) 15825–15835.
- [18] T. Niikura, et al., A tripartite motif protein TRIM11 binds and destabilizes Humanin, a neuroprotective peptide against Alzheimer's disease-relevant insults, *Eur. J. Neurosci.* 17 (2003) 1150–1158.
- [19] K. Ijiri, et al., Increased expression of humanin peptide in diffuse type pigmented villonodular synovitis: implication of its mitochondrial abnormality, *Ann. Rheum. Dis.* 64 (2005) 816–823.
- [20] S. Kariya, M. Hirano, Y. Furiya, K. Sugie, S. Ueno, Humanin detected in skeletal muscles of MELAS patients: a possible new therapeutic agent, *Acta Neuropathol. (Berl)* 109 (2005) 367–372.
- [21] T. Kin, et al., Humanin expression in skeletal muscles of patients with chronic progressive external ophthalmoplegia, *J. Hum. Genet.* 51 (2006) 555–558.
- [22] T. Mamiya, M. Ukai, [Gly¹⁴]-Humanin improved the learning and memory impairment induced by scopolamine in vivo, *Br. J. Pharmacol.* 134 (2001) 1597–1599.
- [23] G. Krejcová, J. Patocka, J. Slaninová, Effect of humanin analogues on experimentally induced impairment of spatial memory in rats, *J. Peptide Sci.* 10 (2004) 636–639.
- [24] J. Miao, et al., S14G-Humanin ameliorates A β 25–25-induced behavioral deficits by reducing neuroinflammatory responses and apoptosis in mice, *Neuropeptides* 42 (2008) 557–567.
- [25] X. Xu, et al., Neuroprotective effect of humanin on cerebral ischemia/reperfusion injury is mediated by a PI3K/Akt pathway, *Brain Res.* 1227 (2008) 12–18.
- [26] F. Anisaka, T. Niikura, T. Arakawa, Y. Kita, The structure analysis of Humanin analog, AGA-(C8R)HNG17, by circular dichroism and sedimentation equilibrium: comparison with the parent molecule, *Int. J. Biol. Macromol.* 43 (2008) 88–93.
- [27] T. Chiba, et al., Development of a femtomolar-acting humanin derivative named colivelin by attaching activity-dependent neurotrophic factor to its N terminus: characterization of Colivelin-mediated neuroprotection against Alzheimer's disease-relevant insults in vitro and in vivo, *J. Neurosci.* 44 (2005) 10252–10261.
- [28] G. Kunesova, et al., The multiple T-maze in vivo testing of the neuroprotective effect of humanin analogues, *Peptides* 29 (2008) 1982–1987.
- [29] T. Chiba, et al., Colivelin prolongs survival of an ALS model mouse, *Biochem. Biophys. Res. Commun.* 343 (2006) 793–798.
- [30] T. Chiba, et al., Evidence for in vivo production of humanin peptide, a neuroprotective factor against Alzheimer's disease-related insults, *Neurosci. Lett.* 324 (2002) 227–231.
- [31] Y. Yamagishi, Y. Hashimoto, T. Niikura, I. Nishimoto, Identification of essential amino acids in Humanin, a neuroprotective factor against Alzheimer's disease-relevant insults, *Peptides* 24 (2003) 585–595.

- [32] K. Terashita, et al., Two serine residues distinctly regulate the rescue function of Humanin, an inhibiting factor of Alzheimer's disease-related neurotoxicity: functional potentiation by isomerization and dimerization, *J. Neurochem.* 85 (2003) 1521–1538.
- [33] D. Mishmar, E. Ruiz-Pesini, M. Brandon, D.C. Wallace, Mitochondrial DNA-like sequences in the nucleus (NUMTs): insights into our African origins and the mechanism of foreign DNA integration, *Hum. Mutat.* 23 (2004) 125–133.
- [34] E. Richly, D. Leister, NUMTs in sequenced eukaryotic genomes, *Mol. Biol. Evol.* 21 (2004) 1081–1084.
- [35] E. Ruiz-Pesini, et al., An enhanced MITOMAP with a global mtDNA mutational phylogeny, *Nucleic Acids Res.* 35 (2007) D823–828.
- [36] T. Niikura, T. Chiba, S. Aiso, M. Matsuoka, I. Nishimoto, Humanin, after the discovery, *Mol. Neurobiol.* 30 (2004) 1–13.
- [37] A. Caricasole, et al., A novel rat gene encoding a Humanin-like peptide endowed with broad neuroprotective activity, *FASEB J.* 16 (2002) 1331–1333.
- [38] W. Kamysz, M. Okroj, E. Lempicka, T. Ossowski, J. Lukasiak, Fast and efficient purification of synthetic peptides by solid-phase extraction, *Acta Chromatographica* 14 (2004) 180–186.
- [39] M. Bodzioch, et al., The microarray expression analysis identifies BAX as a mediator of beta-carotene effects on apoptosis, *Nutr. Cancer* 51 (2005) 226–235.